

Supporting Information

Leclercq et al. 10.1073/pnas.1415174111

SI Methods

Diagnosis of Cirrhosis. Liver biopsy is still regarded as the gold standard for grading and staging liver disease. However, this invasive procedure carries the risk of potential life-threatening complications (e.g., bleeding); therefore, for obvious ethical reasons, liver biopsy cannot be justified in all patients for study purposes. All of the subjects were instead systematically evaluated by blood tests (biochemistry, hematology, coagulation), by gastrointestinal endoscopy (to check for signs of portal hypertension such as esophageal and gastric varices), by liver Doppler-ultrasound (to evaluate the shape of the liver, splenomegaly with collateral intraabdominal venous circulation, or slow or inverted portal venous blood flow), and by measurement of transient liver elastography (Fibroscan). This new noninvasive technique has been designed to quantify liver stiffness, which has been correlated to liver fibrosis grades based on the METAVIR classification system of fibrosis. A validated cutoff has been published, and studies clearly show that this technique is reliable in ruling out significant fibrosis and in confirming cirrhosis (1). Accordingly, we selected only F0 and F1 patients (i.e., absence of significant fibrosis) for the study (2, 3). Liver biopsy was performed only in patients in whom advanced fibrosis/cirrhosis was suspected after noninvasive work-up; these patients were, by definition, excluded from the study.

Gut-Microbiota Analysis by Pyrosequencing and qPCR. Fecal microbiota composition was studied by pyrosequencing of the V1-V2 region of the 16S rRNA gene. The 16S rDNA was amplified by using 27F and 338R primers fused with 454 titanium sequencing adapters. The 338R primers contained unique error-correcting 12-base barcodes that allowed us to tag PCR products from different samples (4). Each sample was amplified in triplicate in a reaction volume of 25 μ L containing 1.5 U of FastStart Taq DNA Polymerase (Roche), 0.2 μ M each primer, and 20 ng of genomic DNA. PCR was carried out under the following conditions: initial denaturation for 3 min at 95 $^{\circ}$ C, followed by 25 cycles of denaturation for 20 s at 95 $^{\circ}$ C, annealing for 20 s at 52 $^{\circ}$ C and elongation for 60 s at 72 $^{\circ}$ C, and a final elongation step for 8 min at 72 $^{\circ}$ C. The amplification of the 16S rDNA was not successful for two control samples, which were therefore excluded from the pyrosequencing analysis. Triplicates were combined, purified with the NucleoSpin Gel and PCR Clean-up kit (Macherey-Nagel), and then quantified by using the Quant-iT PicoGreen dsDNA kit (Invitrogen). Purified PCR products were diluted to a concentration of 20 ng/ μ L and pooled in equal amounts. The pooled amplicons were purified again with the Ampure magnetic purification beads (Agencourt) to remove short amplification products. Sequencing was performed by using 454 GS FLX titanium chemistry at GATC Biotech.

Raw data were quality filtered to remove sequences that were shorter than 200 nucleotides or longer than 1,000 nucleotides, or that contained primer mismatches, ambiguous bases, uncorrectable barcodes, or homopolymer runs in excess of 6 bases. Quality-filtered reads were trimmed of 454 adapter and barcode sequences and analyzed with the software package Quantitative Insights Into Microbial Ecology (QIIME) (5) (version 1.6.0). A total of 517,808 sequences were obtained for the 39 samples (13 controls and 13 AD subjects sampled before and after alcohol withdrawal). Sequences were demultiplexed, and an average of 13,277 sequences were attributed to each sample (range, 6,636–16,482 sequences). Sequences were assigned to operational tax-

onomic units (OTUs) by using UCLUST with a 97% threshold of pairwise identity. The most abundant sequence was picked as representative for each OTU and was given a taxonomic assignment by using the Ribosomal Database Project (RDP) Classifier (6). Representative OTUs were aligned with Pynast (7). Sequences were checked for the presence of chimeras by using ChimeraSlayer, and chimeric sequences were excluded from all downstream analyses. Similarly, sequences that could not be aligned with Pynast were also excluded.

qPCR of 16S rDNA was used to quantify the abundance of selected members of the gut microbiota. The primers used to detect total bacteria, *Bifidobacterium* spp., *Lactobacillus* spp., and *Faecalibacterium prausnitzii* are mentioned in Table S5. PCR amplification was carried out as follows: 10 min at 95 $^{\circ}$ C, followed by 45 cycles of 3 s at 95 $^{\circ}$ C, 26 s at 58 $^{\circ}$ C or 60 $^{\circ}$ C, and 10 s at 72 $^{\circ}$ C. Detection was achieved with the STEP one PLUS instrument and software (Applied Biosystems) using the MESA FAST qPCR MasterMix Plus for SYBR Assay (Eurogentec). BSA was added to samples. Each assay was performed in duplicate in the same run. For construction of standard curves, fivefold dilution series from target species genomic DNA preparations (DSMZ) were applied to the PCR.

Analysis of Volatile Organic Compounds in Fecal Samples by GC-MS.

VOCs from stool samples were analyzed on a gas chromatography-mass spectrometry (GC-MS) quadrupole (Trace GC, Thermoquest; DSQ II, Thermo Electron), which was coupled online to a purge-and-trap system. Before analysis, 125-mg fecal aliquots were suspended in 5 mL of water. Diethyl acetic acid (1.5 mg/L) was added as an internal standard. A magnetic stirrer, sulfuric acid, and a pinch of sodium sulfate were added to the sample to acidify and salt out the solution.

Briefly, VOCs were purged out of the sample with a helium flow [high purity (>99.99%)] at a rate of 40 mL/min for 20 min at 70 $^{\circ}$ C. Consequently, helium was carried over a “dry flow” column (Trap Tenax, Velocity; Interscience) to control moisture transfer, and VOCs were concentrated on a second polar trap column (Trap Vocab, Velocity; Interscience). By raising the temperature to 250 $^{\circ}$ C, the VOCs were desorbed from the column to the injector of the GC, where they were separated on an analytical column (AT Aquawax DA, 30 m \times 0.25 mm i.d., 0.25 μ m film thickness; Grace). The oven starting temperature was 35 $^{\circ}$ C for 1 min and increased by 5 $^{\circ}$ C/min to 100 $^{\circ}$ C and by 10 $^{\circ}$ C/min to 240 $^{\circ}$ C. The final temperature was held constant for 5 min. Masses between m/z 33 and m/z 200 were detected in full-scan mode at 1.5 scans per s. XCalibur software, version 1.4 (SR1; Thermo Electron) was used for automatization of the GC-MS and for data acquisition.

The chromatograms that were obtained were processed by using AMDIS (Automatic Mass Spectral Deconvolution and Identification Software, version 2.71) provided by the US National Institute of Standards and Technology (NIST). This software provides quality matching by using advanced spectral algorithms, adjacent peak deconvolution, and background subtraction, which enable unambiguous identification together with quantitative indication of the metabolite levels. Identification of the metabolites in the samples was achieved by manual visual inspection of the mass spectra of unknown peaks with the NIST library. All compounds were relatively quantified compared with diethyl acetic acid.

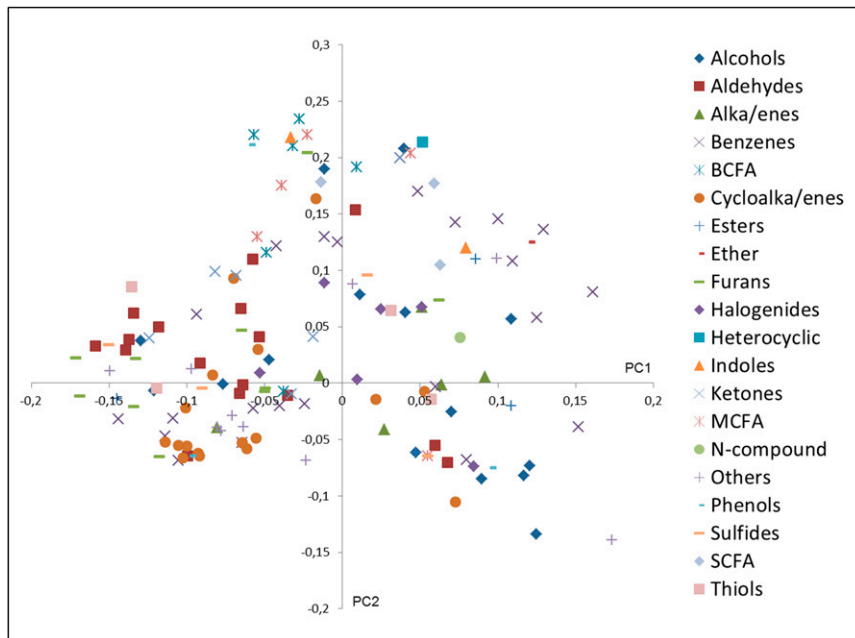
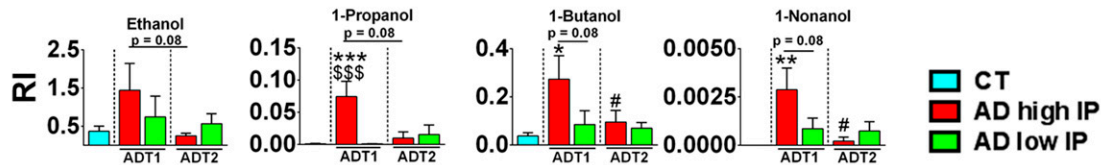
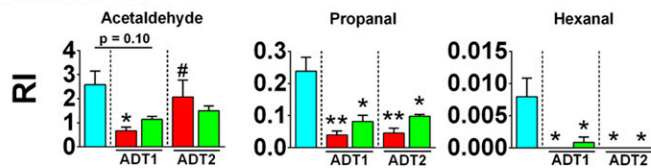


Fig. S3. Loading plot resulting from PLS-DA analysis of metabolite profiles. This plot, showing the metabolites listed according to their chemical class, was used to identify discriminating metabolites.

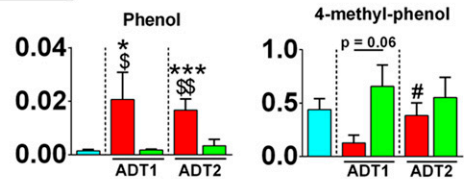
Alcohols A



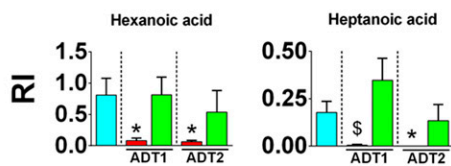
Aldehydes B



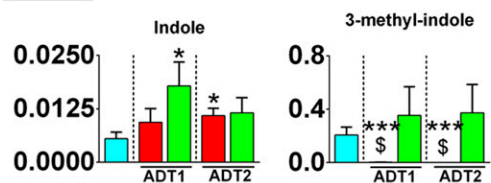
Phenols E



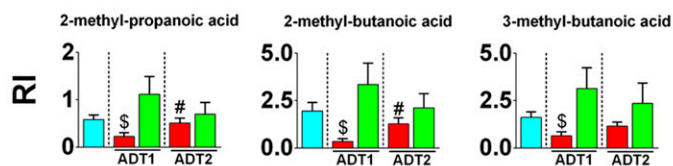
MCFA C



Indoles F



BCFA D



Sulfides G

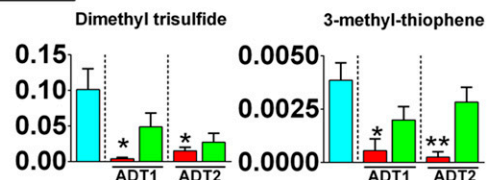


Fig. S4. Volatile organic compounds belonging to the chemical classes (A) alcohols, (B) aldehydes, (C) medium-chain fatty acids (MCFAs), (D) branched-chain fatty acids (BCFAs), (E) phenols, (F) indoles, and (G) sulfides. * $P < 0.05$ compared with CT, ** $P < 0.01$ compared with CT, *** $P < 0.001$ compared with CT, $^{\$}P < 0.05$ AD high IP vs. AD low IP at the same study time, $^{\$\$}P < 0.01$ AD high IP vs. AD low IP at the same study time, $^{\$ \$ \$}P < 0.001$ AD high IP vs. AD low IP at the same study time, $^{\#}P < 0.05$ compared with ADT1 high IP. AD subjects with high IP and low IP are depicted in red and green, respectively. CT subjects are depicted in blue. AD, alcohol-dependent subjects; CT, control subjects; IP, intestinal permeability; RI, relative indices. T1 and T2 refer to the beginning and end of alcohol withdrawal, respectively.

Table S1. Average values of intestinal permeability (IP) in CT and AD subjects at the beginning (T1) and end (T2) of alcohol withdrawal

Time	IP	CT	AD high IP	AD low IP
T1	0–4 h	2.36 ± 0.87	7.81 ± 5.46 ***/\$\$\$	2.58 ± 0.79
	4–24 h	1.08 ± 0.37	2.79 ± 1.73 ***/\$\$\$	0.90 ± 0.26
	0–24 h	1.34 ± 0.43	3.71 ± 2.15 ***/\$\$\$	1.22 ± 0.28
T2	0–4 h	nd	3.26 ± 2.54 \$	1.93 ± 1.11
	4–24 h	nd	1.46 ± 1.01	1.00 ± 0.63
	0–24 h	nd	1.86 ± 1.34	1.23 ± 0.75

Results are expressed as the percentage of the ingested dose of $^{51}\text{Cr-EDTA}$ found in urine normalized for creatinine. Urine was collected for 24 h during two periods that were expected to reflect small-bowel (0–4 h) and colon (4–24 h) permeability. From the total intestinal permeability value at T1, AD patients were split into high IP and low IP groups. Data are means ± SD. *** $P < 0.001$ vs. CT; $^{\$}P < 0.05$ vs. AD low IP; $^{\$ \$ \$}P < 0.001$ vs. AD low IP. AD, alcohol-dependent; CT, control; nd, not defined.

Table S2. Volatile organic compounds found in more than 80% of the CT and AD study subjects

Chemical class	Metabolite	Presence in CT, %	Presence in ADT1, %
Alcohol	1-Butanol	100	100
Aldehyde	Acetaldehyde	100	100
Aldehyde	Propanal	100	100
Aldehyde	Propanal, 2-methyl-	91	85
Aldehyde	Aldehyde RT 19.73	82	100
Aldehyde	Aldehyde RT 22.42	91	85
Aldehyde	Aldehyde RT 23.23	100	100
Benzene	Benzene	82	85
Benzene	Toluene	100	100
Benzene	x-Xylene RT 7.07	91	100
Benzene	Benzene, RT 9.86	100	100
Benzene	Benzene, RT 10.27	82	100
Cycloalkene	Δ-Limonene	100	100
Cycloalkene	3-Cyclohexene-1-methanol, .alpha.,.alpha.4-trimethyl-	91	85
SCFA	Acetic acid	100	100
SCFA	Propanoic acid	100	100
SCFA	Butanoic acid	100	100
BCFA	Propanoic acid, 2-methyl-	100	100
BCFA	Butanoic acid, 3-methyl-	100	100
BCFA	Butanoic acid, 2-methyl-	100	100
BCFA	Pentanoic acid, 4-methyl-	100	85
MCFA	Pentanoic acid	100	100
MCFA	Hexanoic acid	100	100
Ether	Ethyl ether	100	100
Furan	Furan	100	85
Furan	Furan, tetrahydro-	100	92
Halogenide	Trichloromethane	100	92
Halogenide	Bromochloronitromethane	100	100
Halogenide	Methane, tribromo-	91	92
Indole	Indole	100	100
Phenol	Phenol	82	92
Phenol	Phenol, 4-methyl-	100	100
Sulfide	Carbon disulfide	100	100
Sulfide	Disulfide, dimethyl	100	100
Sulfide	Dimethyl trisulfide	100	92
Thiol	3,4-Dimethylthiophene	100	100
Other	Benzaldehyde	100	100
Other	Benzoic acid, 4-ethoxy-, ethyl ester	100	100

Some aldehydes and benzenes were not identified. AD, alcohol-dependent; BCFA, branched-chain fatty acid; CT, control; MCFA, medium-chain fatty acid; RT, retention time (min); SCFA, short-chain fatty acid. T1 refers to the beginning of alcohol withdrawal.

Table S3. Volatile organic compounds found in CT subjects but in less than 10% of alcohol-dependent AD subjects

Chemical class	Metabolite	Presence in CT, %	Presence in ADT1, %
Alcohol	1-Butanol, 2-methyl-	64	0
Aldehyde	Butanal, 3-methyl-	36	<10
Aldehyde	Hexanal	55	<10
Benzene	Benzene, RT 11.26	27	0
Cycloalkane	Cyclopentane, methyl-	27	0
Furan	Furan, 2-ethyl-5-methyl-	27	<10
Ketone	2-Pentanone	27	<10
Thiol	Methanethiol	55	0
Other	Anisole, p-allyl-	36	<10

The metabolite benzene RT 11.26 was not identified. AD, alcohol-dependent; CT, control; RT, retention time. T1 refers to the beginning of alcohol withdrawal.

